Photoacoustics 31 (2023) 100511

Contents lists available at ScienceDirect

Photoacoustics

journal homepage: www.elsevier.com/locate/pacs

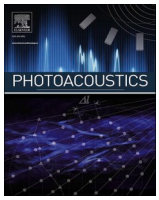

ICG clearance test based on photoacoustic imaging for assessment of human liver function reserve: An initial clinical study

Tingting Qiu [a], Chihan Peng [a], Lin Huang [b,*], Jinge Yang [b], Wenwu Ling [a], Jiawu Li [a], Hongjin Xiang [a], Yan Luo [a,*]

[a] Department of Ultrasound, West China Hospital, Sichuan University, 37 Guoxue Alley, Wuhou District, Chengdu 610041, China
[b] School of Electronic Science and Engineering, University of Electronic Science and Technology of China, No.2006, Xiyuan Ave, West Hi-Tech Zone District, Chengdu 611731, China

ARTICLE INFO

Keywords:
Liver
Indocyanine green
Photoacoustic imaging

ABSTRACT

Liver function reserve (LFR) plays an extensive and important role in patients with liver disease. Indocyanine green (ICG) clearance test is the standard diagnostic approach for LFR evaluation which was performed by spectrophotometry or pulse dye densitometry (PDD). Spectrophotometry is the gold standard, it's invasive and not real-time. PDD is non-invasive, but accuracy of PDD is controversial. Taken spectrophotometry as the reference standard, this study investigated the accuracy of photoacoustic imaging (PAI) method for LFR assessment and compared to PDD in healthy volunteers. The results demonstrated a strong correlation between PAI method and spectrophotometry ($r = 0.9649$, $p < 0.0001$). No significant difference was shown in ICG clearance between PAI and spectrophotometry method (rate constant k1 vs. k2, 0.001158 +−0.00042 vs. 0.001491 +- 0.00045, $p = 0.0727$; half-life t1 vs. t2, 601.2 s vs. 474.4 s, $p = 0.1450$). These results indicated that PAI may be valuable as a noninvasive, accurate diagnostic tool for LFR assessment in human.

1. Introduction

Liver function reserve (LFR) is the sum of remnant functional hepatic cells after liver injury. Hepatitis B or C infections, nonalcoholic fatty liver disease, and long-term alcohol abuse can cause repeated liver injury and progressive liver fibrosis, leading to insufficient LFR or even liver failure [1–3]. LFR assessment plays an extensive and important role in patients with various liver diseases: it can help determine the safe scope of a liver resection or drug regimen and predict prognosis [3–5].

Indocyanine green (ICG), a U.S. Food and Drug Administration (FDA)–approved dye, which can be selectively taken up by hepatic cells, eliminated through bile in its original form without any metabolic change in liver or extrahepatic intake. Due to this exclusive hepatic clearance, an ICG clearance test is the standard diagnostic approach to evaluate LFR, with the dynamic change of blood ICG concentration measured by spectrophotometry or pulse dye densitometry (PDD) [6]. Spectrophotometry is the gold standard, however, it's an invasive, complex and not real-time procedure that demands serial blood sampling [7]. PDD is non-invasive, but it's a blind test without any imaging guidance. Additionally, according to previous study results the accuracy of PDD is controversial [8,9]. Besides the ICG clearance test, a scoring system such as Child-Pugh is widely used for clinical estimation of liver function, but it suffers from low sensitivity and specificity [10]. Computed tomography (CT) volumetry measures liver volume to reflect liver function indirectly, but liver function can't be evaluated directly by CT [11]. Other novel methods such as 99mTc-GSA SPECT and gadoxetic acid-enhance MRI are also being translated and evaluated for LFR assessment in the clinic. However, both are not suitable for frequent screening or real-time monitoring and suffer from poor spatial resolution, high cost, limited availability, and ionizing radiation exposure in the case of SPECT [12,13].

Photoacoustic imaging (PAI) is a non-invasive and non-ionizing technique that provides structural and functional information with high spatial resolution based on optical absorption. PAI has demonstrated its utility for in vivo imaging from organelles to organs [14]. However, clinical application studies of PAI have been traditionally restricted to superficial structures such as breast [15], thyroid [16], arthrosis [17], skin [18] and blood vasculature of extremities [19]. Recent advancements in technology have shown promise for the integration of PAI into the imaging of internal organs such as prostate [20].

* Corresponding authors.
E-mail addresses: lhuang@uestc.edu.cn (L. Huang), yanluo@scu.edu.cn (Y. Luo).

https://doi.org/10.1016/j.pacs.2023.100511
Received 8 August 2022; Received in revised form 8 May 2023; Accepted 10 May 2023
Available online 12 May 2023

Due to the optical absorption of skin and muscles above the liver, PAI studies on the liver were conducted on small animals of fatty liver or liver fibrosis. These studies utilized photoacoustic spectral analysis to evaluate hepatic fat rate or fibrosis severity [21,22]. However, translating these promising results to humans presents a significant challenge due to the deep location of the human liver. Fortunately, when using ICG clearance to evaluate LFR, it is feasible to precisely measure the concentration or clearance of ICG in any blood vessel within the human body subsequent to ICG administration, including the superficial peripheral vessels. Our research team has delineated and authenticated the ICG clearance test utilizing the PAI technique, by employing tissue-mimicking phantoms, in vivo normal and partial hepatectomy rabbit models [23]. The encouraging outcomes obtained from the previous in vitro and in vivo animal studies prompted us to further explore the potential for clinical translation.

In this study, we present a clinical trial of LFR assessment in healthy volunteers by PAI-based ICG clearance test. Taken spectrophotometry as the reference standard, the accuracy of this PAI-based method for LFR assessment was investigated and compared to PDD. Additionally, we demonstrated the use of PAI-derived parameters for describing LFR.

2. Materials and methods

2.1. Study design

The aim of this study was to clinically implement the PAI-based ICG clearance test for LFR assessment, based on the results of our previously published phantom and animal studies. Between August 10, 2020, and September 1, 2020, 16 healthy volunteers without any history of liver disease were recruited. The exclusion criteria were as follows: (1) a history of iodine allergy (n = 1), (2) hemolysis of blood sample (n = 2), and (3) unexpected movement of the elbow or nose, such as sneezing (n = 1). In total, 12 healthy volunteers (man = 6, woman = 6) were included in the final analysis. These volunteers were intravenously administered ICG and received PAI, PDD and spectrophotometry simultaneously. This initial clinical trial was approved by Ethics Committee on Biomedical research, University of Electronic Science and Technology of China. Informed consent was obtained from all participating volunteers.

2.2. Patient data

The demographic data and blood work results were displayed in Table 1.

2.3. Photoacoustic imaging (PAI) system

Fig. 1 depicts the schematic representation of the PAI system utilized for imaging human blood vessels. The PAI system is based on a Q-switched Nd:YAG - pumped optical parameter oscillator (Surelite, Continuum, California), a 128-element hollow concave array (center frequency:2.0 MHz, with a bandwidth of 80%, element size: The elements are evenly distributed and have a pitch of 1.6 mm and a height of 20 mm. The central region of the array, consisting of 32 elements (from the 49th to the 80th element), is hollow and contains two segments that are 1.5 * 5 mm each. This allows for the insertion of the linear transducer array. The concave array has a cylindrical focal length of 70 mm in the y − z plane, and the radius of curvature in the x − y plane is chosen to be 65 mm, enabling 180° imaging coverage, ULSO TECH CO., LTD, China) [24]. The laser provides tunable laser pulses from 700 to 960 nm at a repetition rate of up to 20 Hz. The output laser light is coupled into a custom-made fiber buddle [23]. The output shape of the fiber bundle is a rectangular region with a 10 mm × 5 mm area. The maximum light fluence from the fiber bundle at 805 nm is estimated to be 10 mJ/cm^2 (within the safety limit of the American National Standards Institute regulations) in this study. The PA signals emitted by the blood and ICG are collected by the hollow concave array and first transmitted into a homemade 128-to-64 multiplexing system, then amplified by a custom-made 64-channel preamplifier. The PA signals were finally averaged for 10 times and recorded by a 64-channel acquisition system with two 32-channel data acquisition cards (DAQ, 5752B, NI. Inc., USA) at a sampling rate of 50 MS/s. Under 20 Hz working frequency of the laser, the whole data acquisition time was about 1 s. PA image was recovered using a delay-and-sum algorithm in Matlab (Mathworks Inc., Natic, MA) [25].

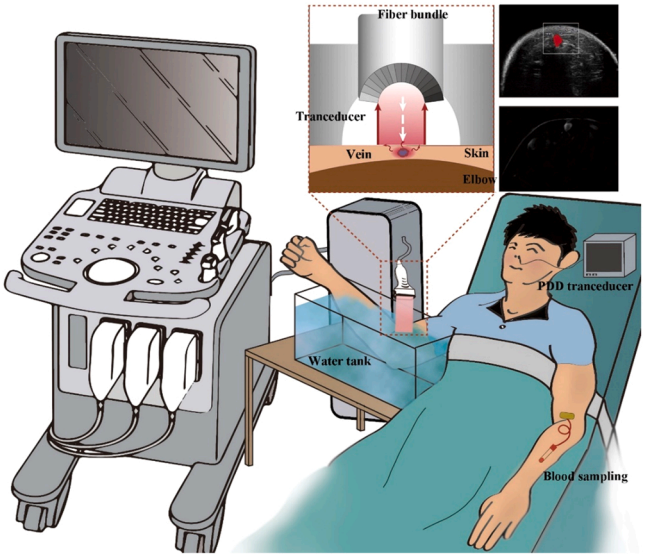

Fig. 1. Schematic of the experiment system.

Table 1
Demographic data and blood work of volunteers.

Characteristic	Value
Gender, n (%)	
male	6 (50)
female	6 (50)
Age (mean±sd, years old)	30.8 ± 6.7
Blood work (mean±sd)	
hemoglobin (Hb, g/L)	141.5 ± 16.0
red blood cell (RBC) count (10^12/L)	4.7 ± 0.6
platelet (PLT) count (10^9/L)	227.5 ± 65.4
alanine aminotransferase (ALT, IU/L)	21.3 ± 12.5
aspartate aminotransferase (AST, IU/L)	21.3 ± 6.0
albumin (ALB, g/L)	47.7 ± 3.0
total bilirubin (TB, μmol/L)	11.8 ± 7.6
direct bilirubin (DB, μmol/L)	2.8 ± 1.2

2.4. ICG clearance test by spectrophotometry

As illustrated in Fig. 1, the volunteer was in supine position with his left arm extended. The ICG (Dandong Yi Chuang, Liaoning, China) was dissolved in distilled water to achieve a concentration of 5 mg/ml immediately prior to administration. A dose of 0.1 ml/kg ICG solution was injected into the left median cubital vein (MCV) followed by a 5 ml saline flush over a period of 10 s. Blood samples were collected at the following designated time intervals: 0 s (prior to ICG injection), 30 s, 60 s, 100 s, 180 s, 300 s, 480 s, 600 s, 760 s, 900 s after ICG injection through the left MCV into an anticoagulant vacuum tube. Subsequently, the collected blood was centrifuged at 3000r/m for a duration of 10 min. The absorbance of each plasma sample was then measured at 805 nm by means of a spectrophotometer (ZB006, Shanghai INESA Scientific Instrument Co., Ltd, China).

2.5. ICG clearance test by PAI

As shown in Fig. 1., the volunteer was in supine position. Right arm was outstretched. Initially, B-mode ultrasound (Resona 9, Mindray, China) was utilized to identify the location of the right MCV, and the resulting transverse ultrasound section of the right MCV is presented in Fig. 2A. Following this, the identified location was marked, and the right arm was submerged in a water tank. The PAI imaging probe was then positioned on the marked right MCV, and the transverse section of the marked right MCV was clearly visualized through PAI, as demonstrated in Fig. 2B. The white dashed box delineated the region of interest (ROI) for the subsequent analysis.

PAI scanning of the marked right MCV at a wavelength of 805 nm was conducted for a duration of 15 min. The acquisition rate was set at 0.5 frames per second. Prior to the injection of ICG, a baseline PAI scan of the target MCV was conducted for a period of 10 s. Subsequently, the PA image was continuously acquired for an additional 900 s following the administration of ICG. Owing to the rapid changes in ICG concentration at the beginning and the slower changes in concentration in the later stages [6,7,9,23], we acquired PA images at 5-second intervals during the first 180 s, followed by 10-second intervals in the subsequent stage.

For image processing, firstly, the delay and sum algorithm based on MATLAB is used to obtain PA images (Fig. 3) of each frame. Due to the presence of motion artifacts during the experiment, image registration is required. ImageJ software is used to perform rigid registration on the images to obtain a series of new images. Then, taking the first image as a reference and combining it with ultrasound imaging results, a professional ultrasound clinician manually selects the vascular region for annotation and calculates the total sum of pixel values in the selected region. The same vascular region is then annotated and calculated for all frame images in turn. Since the obtained PA vascular images include information on both oxygenated and deoxygenated hemoglobin components, when calculating the ICG concentration changes, the signals collected 10 s prior to ICG injection are averaged as a baseline. Then, all vascular signals after ICG injection are subtracted from this baseline to obtain the required values for calculating the ICG concentration changes, and the curve of ICG concentration changes over time after ICG administration is plotted in Fig. 4.

2.6. ICG clearance test by PDD

The instrument used for measuring blood ICG concentration after intravenous injection was the PDD (DDG-3300 K, Nihon Kohden, Tokyo, Japan). A pulse-by-pulse monitoring of blood ICG concentrations was performed through an optical probe attached to the volunteer's nasal wing. The obtained blood ICG concentrations were automatically converted to logarithmic scale, and linearly regressed against time with the method of least squares, from 2.5 min (when ICG was assumed to completely mixed with blood) through 5.5 min after the mean transit time, to acquire the slope of the regression line. The elimination rate constant (k value) and half-life were automatically computed from the time course of blood ICG concentration.

2.7. Statistical analysis

Statistical analysis and graphical display of data were performed using GraphPad software (version 8.00; GraphPad Software, San Diego, CA, USA). Continuous variables were given as mean and standard deviation (sd) or median and interquartile range (IQR). Similar to previous study [23], averaged PA signal in the MCV were normalized as the relative photoacoustic signal intensity (PSIre) to reflect the ICG concentration change as follows:

$$PSI_{re}(t) = \frac{PSI(t) - PSI_{base}}{PSI_{base}} \quad (1)$$

In order to quantify the kinetics of PSI_{re} change after the ICG administration, an exponential decay model [26] was used as follows:

$$PSI_{re}(t) = PSI_{re}(0)e^{-kt} \quad (2)$$

k is the elimination rate constant, expressed in reciprocal of the X axis time units. Half-life is in the time units of the X axis. It is computed as ln (2)/k.

Comparison between groups (PAI versus Spectrophotometry, PDD versus Spectrophotometry) were conducted using unpaired t-test or unpaired t-test with Welch's correction when standard deviations were not equal. Pearson correlation test was used for correlation analysis. A value of $p < 0.05$ was considered statistically significant.

3. Results

3.1. Correlation between PAI and spectrophotometry

A peak of high intensity was observed after the injection of ICG and gradually decreased over time, as depicted in Fig. 4. A strong correlation was demonstrated between the temporal photoacoustic signal (PAS) in vivo and the absorbance of blood samples in vitro ($r = 0.9649$, $p < 0.0001$).

3.2. Difference in rate constant and half-life between PAI and spectrophotometry

As demonstrated in Fig. 5, no significant difference was shown in ICG clearance between PAI and spectrophotometry method (rate constant k1 vs. k2, 0.001158 ± 0.00042 vs. 0.001491 ± 0.00045, $p = 0.0727$; half-life t1 vs. t2, 601.2 s (25% percentile: 506.2 s, 75% percentile:750.2 s) vs. 474.4 s (25% percentile: 366.4 s, 75% percentile:664.2 s), $p = 0.1450$).

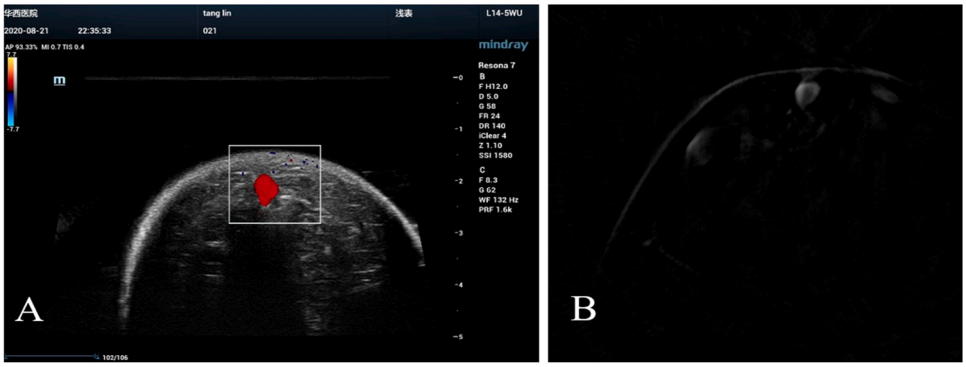

Fig. 2. Ultrasound A and photoacoustic B images of the volunteer's blood vessel (indicated by white dashed box).

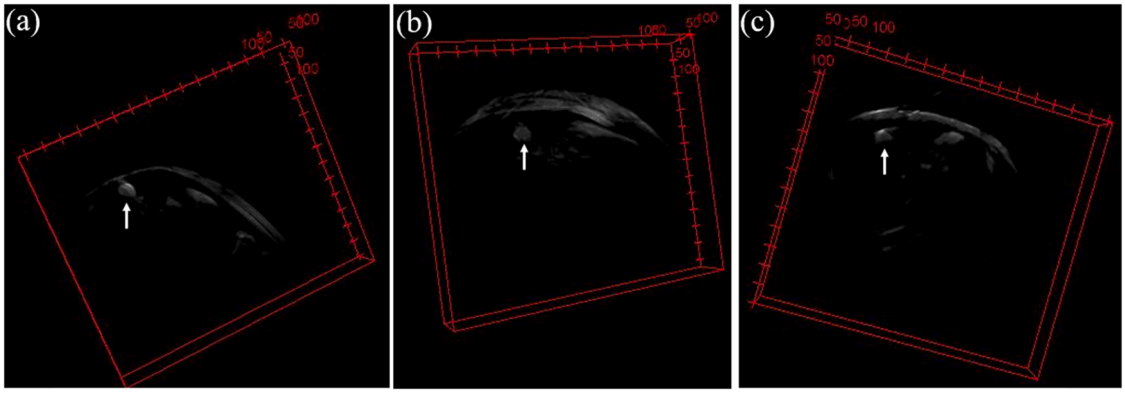

Fig. 3. Registered PA images of the volunteer's blood vessel. (indicated by white arrows).

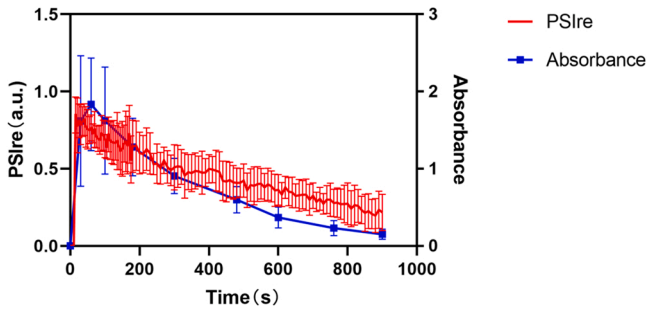

Fig. 4. The in vivo PAI data was collected from 12 healthy volunteers, while in vitro absorbance measurement was performed using blood sample. PSI measured in vivo (red line with error bars), and absorbance estimated in vitro by spectrophotometer (blue line with blue cube and error bars). ICG = indocyanine green, PAS= photoacoustic signal, PAI = photoacoustic imaging, PSIre=relative photoacoustic signal intensity.

3.3. Difference in rate constant and half-life between PDD and spectrophotometry

As illustrated in Fig. 6, a significant difference was observed in ICG clearance between the PDD and Spectro method (rate constant k3 vs. k2, 0.004604 ± 0.00073 vs. 0.001491 ± 0.00045, $p < 0.0001$; half-life t3 vs. t2, 156.0 s (25% percentile: 133.5 s, 75% percentile:174.0 s) vs. 474.4 s (25% percentile: 366.4 s, 75% percentile:664.2 s), $p < 0.0001$).

4. Discussion

ICG clearance test has been used as a LFR test to evaluate patient outcomes, as a prognostic marker and as diagnostic tool in mainly two areas: in liver surgery (including hepatic resection and liver transplantation) and in critically ill patients (in patients with or without liver failure) [1–5]. A range of techniques, invasive or non-invasive, are available for assessing ICG elimination. These techniques yield various derived values that quantify ICG elimination, including the elimination rate constant (k), which reflects the decay rate of ICG. The half-life provides the time elapsed from the peak concentration of ICG to the point at which the concentration has decreased to half of its peak value. ICG retention rate at 15 min (ICGR15), which is the circulatory retention of ICG during the first 15 min following bolus injection, expressed as a percentage. ICGR15 derived from PDD method is a common value for LFR assessment. However, the accuracy of this value for predicting post-hepatectomy liver failure has been called into question [9]. It is recommended that additional methods be considered for a comprehensive assessment of LFR. Values obtained through invasive techniques, such as spectrophotometry, including elimination rate constant and half-life, may provide more reliable indicators of remnant liver function.

Our previous phantom and animal study has shown that PAI was useful for monitoring ICG clearance in normal and partial hepatectomy rabbits [23]. Other previous studies have demonstrated a mono-exponential decline in ICG plasma concentration over time after low doses (0.5 mg/kg) were administered to both humans and laboratory animals, as measured by spectrophotometry or high-pressure liquid chromatography [27–30]. These findings are in agreement with our observations obtained through PAI in both animal and human subjects. Recent studies demonstrated the utility of PAI in reflecting LFR in partial hepatectomy or liver fibrosis mouse models, results of which showed the significant difference of PAI-related parameters between the control and disease model groups [26,31].

Due to the depth limitations of PAI, direct imaging of liver tissue using PAI in humans is challenging. Nevertheless, this issue has been

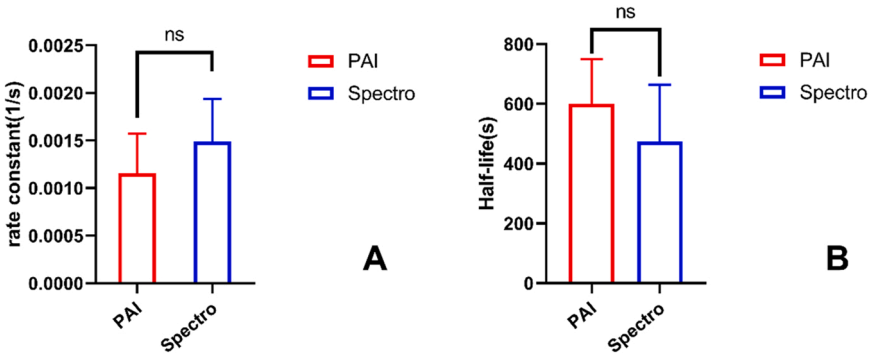

Fig. 5. Difference analysis between the PAI and spectrophotometry method. A. Rate constant k of ICG clearance between PAI and Spectro. B. half-life of ICG clearance between PAI and Spectro. ICG= indocyanine green, PAI=photoacoustic imaging, Spectro=spectrophotometer ns= not significant.

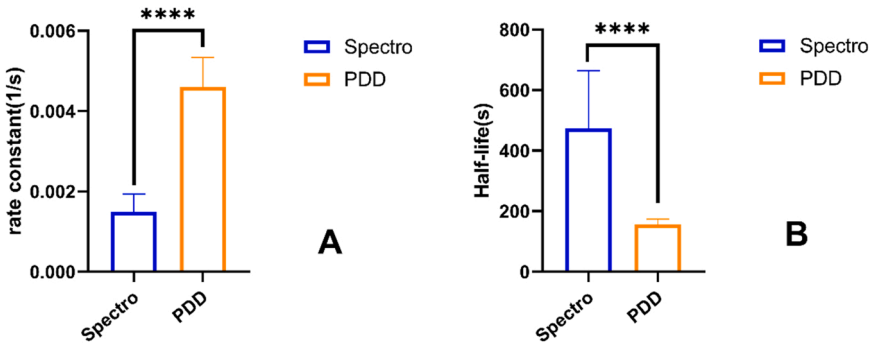

Fig. 6. Difference analysis between the PDD and Spectro method. A. Rate constant k of ICG clearance between PDD and Spectro. B. half-life of ICG clearance between PDD and Spectro. ICG= indocyanine green, PDD=pulse dye densitometry, Spectro=spectrophotometer, * ** *=$p < 0.0001$.

circumvented by conducting peripheral superficial vessel scanning, which has demonstrated promising potential for translating PAI to human use for assessing LFR. This study aimed to achieve clinical translation of real-time monitoring of ICG clearance via peripheral vessels using PAI for assessing LFR in humans. The crucial functional parameters, namely the elimination rate constant (k) and half-life (t1/2) of liver function obtained through PAI, showed no significant difference compared to the gold standard method of spectrophotometry ($p = 0.0727$, $p = 0.1450$ respectively). A strong positive correlation was observed between temporal photoacoustic signal (PAS) obtained by PAI in vivo and absorbance of blood samples in vitro measured by spectrophotometry ($r = 0.9649$, $p < 0.0001$). However, the elimination rate constant (k) and the half-life (t1/2) of ICG clearance calculated by PDD significantly differed from those measured by spectrophotometry ($p < 0.0001$ for both). When compared to spectrophotometry as the accepted standard, the PAI method exhibited a high level of accuracy in assessing LFR among healthy volunteers. However, the elimination rate constant (k) and half-life (t1/2) measurements obtained through PDD demonstrated significant deviations from the results obtained through the gold standard. A similar result was reported by T. Imai, K et al., who presented evidence of poor consistency between PDD and spectrophotometry [9]. PDD is a blind-test based on two-wavelength near-infrared light (805 and 890 nm) in association with pulse oximetry to compute the arterial blood concentration ratio of ICG to hemoglobin (Hb). A slight movement of tested body parts, such as the nose or fingers, can result in inaccurate readings. Furthermore, various factors, including hemoglobin concentration, perivascular tissue, and weak arterial pulse, can also affect the precision of PDD. Additionally, the algorithm utilized by PDD for calculating ICG clearance parameters differs from that of spectrophotometry and PAI [8,9]. Therefore, the aforementioned factors may explain the disparity observed between PDD and spectrophotometry measurement outcomes.

Our study encountered several limitations. Firstly, it should be noted that the ICG clearance test is a comprehensive evaluation of liver function. However, the ability to assess functional heterogeneity among various hepatic segments using this method is restricted. Secondly, although the MCV was discernible through both PA and ultrasound imaging, it is imperative to develop a hybrid photoacoustic/ultrasound imaging platform to enable precise image co-registration for human implementation. Lastly, a prospective clinical study involving a substantial population, including patients, should be undertaken to provide further validation.

5. Conclusions

This study has demonstrated a strong correlation between photoacoustic imaging (PAI) and the gold standard spectrophotometry method for ICG clearance testing. Additionally, the accuracy of PAI was found to be superior to that of pulse dye densitometry.

Declaration of Competing Interest

The authors declare that they have no known competing financial interests or personal relationships that could have appeared to influence the work reported in this paper.

Data Availability

The data that has been used is confidential.

Acknowledgments

This work was supported by the National Natural Science Foundation of China (82001833).

We thank Professor. Zhe Wu from University of Electronic Science and Technology of China and Huabei Jiang from University of South Florida for professional advice in the preparation of the article.

References

[1] J.K. Heimbach, L.M. Kulik, R.S. Finn, C.B. Sirlin, M.M. Abecassis, L.R. Roberts, A. X. Zhu, M.H. Murad, J.A. Marrero, AASLD guidelines for the treatment of hepatocellular carcinoma, Hepatology (2018), https://doi.org/10.1002/hep.29086.

[2] C.S. of I.D.C.M.A. Liver Failure and Artificial Liver Group, C.S. of H.C.M.A. Severe Liver Disease and Artificial Liver Group, [Guideline for diagnosis and treatment of liver failure]., Zhonghua Gan Zang Bing Za Zhi. 27 (2019) 18–26. https://doi.org/10.3760/cma.j.issn.1007–3418.2019.01.006.

[3] European Association for the Study of the Liver. Electronic address: easloffice@easloffice.eu, European Association for the Study of the Liver, EASL Clinical Practice Guidelines for the management of patients with decompensated cirrhosis., J Hepatol. 69 (2018) 406–460. https://doi.org/10.1016/j.jhep.2018.03.024.

[4] H. Imamura, K. Sano, Y. Sugawara, N. Kokudo, M. Makuuchi, Assessment of hepatic reserve for indication of hepatic resection: decision tree incorporating indocyanine green test, J. Hepato-Biliary-Pancreat. Surg. (2005), https://doi.org/10.1007/s00534-004-0965-9.

[5] Y. Seyama, N. Kokudo, Assessment of liver function for safe hepatic resection, Hepatol. Res. (2009), https://doi.org/10.1111/j.1872-034X.2008.00441.x.

[6] P. Ott, Hepatic elimination of indocyanine green with special reference to distribution kinetics and the influence of plasma protein binding, Pharm. Toxicol. (1998), https://doi.org/10.1111/j.1600-0773.1998.tb01945.x.

[7] C.K. Svensson, D.J. Edwards, D. Lalka, P.M. Mauriello, E. Middleton, Comparison of chromatographic and spectrophotometric analysis of indocyanine green in plasma following administration of multiple doses to humans, J. Pharm. Sci. (1982), https://doi.org/10.1002/jps.2600711134.

[8] G.G. Lockwood, N.L.S. Fung, J.G. Jones, Evaluation of a computer program for non-invasive determination of pulmonary shunt and ventilation-perfusion mismatch, J. Clin. Monit. Comput. (2014), https://doi.org/10.1007/s10877-014-9554-x.

[9] T. Imai, K. Takahashi, F. Goto, Y. Morishita, Measurement of blood concentration of indocyanine green by pulse dye densitometry - comparison with the conventional spectrophotometric method, J. Clin. Monit. Comput. (1998), https://doi.org/10.1023/A:1009948128543.

[10] Y.Y. Wang, X.H. Zhao, L. Ma, J.Z. Ye, F.X. Wu, J. Tang, X.M. You, B. de Xiang, L. Q. Li, Comparison of the ability of Child-Pugh score, MELD score, and ICG-R15 to assess preoperative hepatic functional reserve in patients with hepatocellular carcinoma, J. Surg. Oncol. (2018), https://doi.org/10.1002/jso.25184.

[11] M.C. Lim, C.H. Tan, J. Cai, J. Zheng, A.W.C. Kow, CT volumetry of the liver: where does it stand in clinical practice, Clin. Radiol. (2014), https://doi.org/10.1016/j.crad.2013.12.021.
[12] M. Nakagawa, T. Namimoto, K. Shimizu, K. Morita, F. Sakamoto, S. Oda, T. Nakaura, D. Utsunomiya, S. Shiraishi, Y. Yamashita, Measuring hepatic functional reserve using T1 mapping of Gd-EOB-DTPA enhanced 3T MR imaging: a preliminary study comparing with 99mTc GSA scintigraphy and signal intensity based parameters, Eur. J. Radio. 92 (2017) 116–123, https://doi.org/10.1016/j.ejrad.2017.05.011.
[13] Y. Mizutani, T. Hirai, S. Nagamachi, A. Nanashima, K. Yano, K. Kondo, M. Hiyoshi, N. Imamura, T. Terada, Prediction of posthepatectomy liver failure proposed by the international study group of liver surgery: residual liver function estimation with 99mtc-galactosyl human serum albumin scintigraphy, Clin. Nucl. Med 43 (2018) 77–81, https://doi.org/10.1097/RLU.0000000000001913.
[14] L. v Wang, S. Hu, Photoacoustic tomography: In vivo imaging from organelles to organs, Science (2012) (1979), https://doi.org/10.1126/science.1216210.
[15] X.L. Deán-Ben, T.F. Fehm, M. Gostic, D. Razansky, Volumetric hand-held optoacoustic angiography as a tool for real-time screening of dense breast, J. Biophotonics 9 (2016) 253–259, https://doi.org/10.1002/jbio.201500008.
[16] M. Yang, L. Zhao, X. He, N. Su, C. Zhao, H. Tang, T. Hong, W. Li, F. Yang, L. Lin, B. Zhang, R. Zhang, Y. Jiang, C. Li, Photoacoustic/ultrasound dual imaging of human thyroid cancers: an initial clinical study, Biomed. Opt. Express 8 (2017) 3449, https://doi.org/10.1364/boe.8.003449.
[17] J.R. Rajian, X. Shao, D.L. Chamberland, X. Wang, Characterization and treatment monitoring of inflammatory arthritis by photoacoustic imaging: a study on adjuvant-induced arthritis rat model, Biomed. Opt. Express 4 (2013) 900–908, https://doi.org/10.1364/BOE.4.000900.
[18] A. Hariri, F. Chen, C. Moore, J. v Jokerst, Noninvasive staging of pressure ulcers using photoacoustic imaging, Wound Repair Regen. 27 (2019) 488–496, https://doi.org/10.1111/wrr.12751.
[19] P. Wray, L. Lin, P. Hu, L. v Wang, Photoacoustic computed tomography of human extremities, J. Biomed. Opt. 24 (2019) 1–8, https://doi.org/10.1117/1.JBO.24.2.026003.
[20] S.-R. Kothapalli, G.A. Sonn, J.W. Choe, A. Nikoozadeh, A. Bhuyan, K.K. Park, P. Cristman, R. Fan, A. Moini, B.C. Lee, J. Wu, T.E. Carver, D. Trivedi, L. Shiiba, I. Steinberg, D.M. Huland, M.F. Rasmussen, J.C. Liao, J.D. Brooks, P.T. Khuri-Yakub, S.S. Gambhir, Simultaneous transrectal ultrasound and photoacoustic human prostate imaging, Sci. Transl. Med 11 (2019), https://doi.org/10.1126/scitranslmed.aav2169.
[21] G. Xu, Z.-X. Meng, J.D. Lin, J. Yuan, P.L. Carson, B. Joshi, X. Wang, The functional pitch of an organ: quantification of tissue texture with photoacoustic spectrum analysis, Radiology 271 (2014) 248–254, https://doi.org/10.1148/radiol.13130777.
[22] P.J. van den Berg, R. Bansal, K. Daoudi, W. Steenbergen, J. Prakash, Preclinical detection of liver fibrosis using dual-modality photoacoustic/ultrasound system, Biomed. Opt. Express 7 (2016) 5081–5091, https://doi.org/10.1364/BOE.7.005081.
[23] T. Qiu, J. Yang, T. Pan, C. Peng, H. Jiang, Y. Luo, Assessment of liver function reserve by photoacoustic tomography: a feasibility study, Biomed. Opt. Express 11 (2020) 3985–3995, https://doi.org/10.1364/BOE.394344.
[24] X. Wang, L. Huang, Z. Chi, H. Jiang, Integrated thermoacoustic and ultrasound imaging based on the combination of a hollow concave transducer array and a linear transducer array, Phys. Med Biol. 66 (2021), https://doi.org/10.1088/1361-6560/abfc91.
[25] Z. Zheng, L. Huang, H. Jiang, Label-free thermoacoustic imaging of human blood vessels in vivo, Appl. Phys. Lett. 113 (2018), 253702, https://doi.org/10.1063/1.5054652.
[26] N. Brillant, M. Elmasry, N.C. Burton, J.M. Rodriguez, J.W. Sharkey, S. Fenwick, H. Poptani, N.R. Kitteringham, C.E. Goldring, A. Kipar, B.K. Park, D.J. Antoine, Dynamic and accurate assessment of acetaminophen-induced hepatotoxicity by integrated photoacoustic imaging and mechanistic biomarkers in vivo, Toxicol. Appl. Pharmacol. (2017), https://doi.org/10.1016/j.taap.2017.07.019.
[27] C.M. Leevy, J. Bender, Physiology of dye extraction by the liver: comparative studies of sulfobromophthalein and indocyanine green, Ann. N. Y Acad. Sci. 111 (1963) 161–176, https://doi.org/10.1111/j.1749-6632.1963.tb36956.x.
[28] J.J. Thiessen, P.L. Rappaport, J.G. Eppel, Indocyanine green pharmacokinetics in the rabbit, Can. J. Physiol. Pharm. 62 (1984) 1078–1085, https://doi.org/10.1139/y84-180.
[29] K. Stoeckel, P.J. McNamara, A.J. McLean, P. duSouich, D. Lalka, M. Gibaldi, Nonlinear pharmacokinetics of indocyanine green in the rabbit and rat, J. Pharm. Biopharm. 8 (1980) 483–496, https://doi.org/10.1007/BF01059547.
[30] R. Heintz, C.K. Svensson, K. Stoeckel, G.J. Powers, D. Lalka, Indocyanine green: pharmacokinetics in the rabbit and relevant studies of its stability and purity, J. Pharm. Sci. 75 (1986) 398–402, https://doi.org/10.1002/jps.2600750417.
[31] J. Lv, Y. Xu, L. Xu, L. Nie, Quantitative functional evaluation of liver fibrosis in mice with dynamic contrast-enhanced photoacoustic imaging, Radiology 300 (2021) 89–97, https://doi.org/10.1148/radiol.2021204134.

Tingting Qiu is currently a doctor in Department of Ultrasound, West China Hospital, Sichuan University. She received her Ph.D. degree in 2018 from Sichuan University. She completed her post-doctoral fellowship in 2021. Her research mainly focuses on the liver ultrasonography and the clinical application of photoacoustic imaging.

Chihan Peng is currently a doctor in Department of Ultrasound, West China Hospital, Sichuan University. He received his Ph.D. degree in 2019 from Sichuan University. He completed his post-doctoral fellowship in 2022. His research mainly focuses on the liver ultrasonography and interventional ultrasound.

Lin Huang is an Associate Professor of School of Electronic Science and Engineering at University of Electronic Science and Technology of China. He received his Ph.D. in 2015 from University of Electronic Science and Technology of China with expertise in thermoacoustic imaging.

Jinge Yang completed his B.S. and Ph.D. in Electrical Engineering at University of Science and Electronics of China (UESTC) in 2013 and 2019, respectively. His research interests are photoacoustic biomedical imaging techniques and their clinical applications.

Wenwu Ling is an Associate Professor of Department of Ultrasound, West China Hospital, Sichuan University. He graduated from Sichuan University in 2019 with Ph.D. degree. He has been engaged in clinical and scientific research in ultrasound. His research mainly focuses on the contrast-enhanced ultrasound and elastography of abdominal diseases.

Jiawu Li is currently a doctor in Department of Ultrasound, West China Hospital, Sichuan University. He received his Ph.D. degree in 2018 from Sichuan University. He completed his post-doctoral fellowship in 2021. His research mainly focuses on the liver ultrasonography and the clinical application of thermoacoustic imaging.

Hongjin Xiang is currently a doctoral student in Department of Ultrasound, West China Hospital, Sichuan University. She received her bachelor degree from Sichuan University in 2017. Her research mainly focuses on the liver ultrasonography and the application of thermoacoustic imaging for the liver disease.

Yan Luo is currently the director and a Professor of Department of Ultrasound, West China Hospital, Sichuan University. She has been engaged in clinical and scientific research in ultrasound. Her current research interests include ultrasonography for abdominal diseases (especially liver diseases) and emerging imaging technologies.